HHS Public Access

Author manuscript

J Perinat Med. Author manuscript; available in PMC 2018 June 05.

Published in final edited form as:

J Perinat Med. 2015 March ; 43(2): 209–220. doi:10.1515/jpm-2014-0268.

MR imaging of the fetal brain at 1.5T and 3.0T field strengths: comparing specific absorption rate (SAR) and image quality

Uday Krishnamurthy[1,2], **Jaladhar Neelavalli**[1,2,*], **Swati Mody**[1], **Lami Yeo**[3,4], **Pavan K. Jella**[1], **Sheena Saleem**[1], **Steven J. Korzeniewski**[3,4,5], **Maria D. Cabrera**[1], **Shadi Ehterami**[1], **Ray O. Bahado-Singh**[6], **Yashwanth Katkuri**[1], **Ewart M. Haacke**[1,2], **Edgar Hernandez-Andrade**[3,4], **Sonia S. Hassan**[3,4], and **Roberto Romero**[3,5,7]

[1]Department of Radiology, Wayne State University School of Medicine, Detroit, MI, USA

[2]Department of Biomedical Engineering, College of Engineering, Wayne State University, Detroit, MI, USA

[3]Perinatology Research Branch, NICHD/NIH/DHHS, Bethesda, MD, and Detroit, MI, USA

[4]Department of Obstetrics and Gynecology, Wayne State University School of Medicine, Detroit, MI, USA

[5]Department of Epidemiology and Biostatistics, Michigan State University, East Lansing, Michigan; USA

[6]Department of Obstetrics and Gynecology, William Beaumont School of Medicine, Oakland University, Rochester, MI, USA

[7]Department of Obstetrics and Gynecology, University of Michigan, Ann Arbor, MI, USA

Abstract

Objective—1) To evaluate the feasibility of fetal brain magnetic resonance imaging (MRI) using a fast spin echo sequence at 3.0T field strength with low radio frequency (rf) energy deposition (as measured by specific absorption rate – SAR) than 1.5T; 2) and to compare image quality, tissue contrast and conspicuity between 1.5T and 3.0T MRI.

Methods—T2 weighted images of the fetal brain at 1.5T were compared to similar data obtained in the same fetus using a modified sequence at 3.0T. Quantitative whole body SAR and normalized image signal to noise ratio (SNR); and a nominal scoring scheme based evaluation of diagnostic image quality and tissue contrast & conspicuity for specific anatomical structures in the brain, were compared between 1.5T and 3.0T.

Results—12 pregnant women underwent both 1.5T and 3.0T MRI examinations. The image SNR was significantly higher ($p=0.03$) and whole body SAR was significantly lower ($p < 0.0001$) for

Correspondence: Jaladhar Neelavalli, Department of Radiology, Wayne State University School of Medicine, 4201 St. Antoine, Detroit, MI, 48201, USA, Tel.: +1 313-993-8610, Fax: +1 313-745-9182, jneelava@med.wayne.edu.

Disclosure/Conflicts of Interest:

The authors have no conflicts of interest.

Disclosure

The authors report no conflicts of interest.

images obtained at 3.0T compared to 1.5T. All cases at both field strengths were scored as having diagnostic image quality. Images from 3.0T MRI (compared to 1.5T) were: 1) equal (57%; 21/37) or superior (35%; 13/37) for tissue contrast; and 2) equal (61%; 20/33) or superior (33%, 11/33) for conspicuity.

Conclusion—It is possible to obtain fetal brain images with higher resolution and better SNR at 3.0T with simultaneous reduction in SAR compared to 1.5T. Images of the fetal brain obtained at 3.0T demonstrated superior tissue contrast and conspicuity compared to 1.5T.

Keywords

fetal imaging; radio frequency energy; specific absorption rate; signal to noise; fetal MRI; 3.0T

INTRODUCTION

While ultrasound has been the primary modality used in prenatal diagnosis the role of magnetic resonance imaging (MRI) in fetal diagnostic evaluation is increasing [1]. Fetal MRI has multiple advantages over ultrasound in this field.[2–36] Such advantages include: 1) improved soft tissue contrast and characterization[4, 21, 37–39]; 2) access to functional data [e.g. diffusion weighted imaging (DWI),[40–48] perfusion weighted imaging (PWI)[12, 32, 49, 50], blood oxygenation dependent (BOLD),[51–55] MR spectroscopy (MRS)[10, 56–65]]; and 3) larger field of view (FOV). Fetal MRI has been shown to be useful in diagnosis of fetal pathologies [66–68]. In particular, fetal MRI has been shown to be superior to ultrasound in evaluating the fetal central nervous system.[4–7, 16, 17, 69–77]

Three decades have passed since the first application of MRI in the human pregnancy.[78] Currently, 1.5 Tesla (T) is the field strength of choice for MRI in pregnancy, although fetal MR imaging at 3.0T has also been reported in several studies.[55, 73, 79–82] Adult, pediatric, and neonatal populations routinely undergo clinical MR examinations at 3.0T.[83–86] The major advantage of 3.0T MRI (vs. 1.5T) is the increased signal to noise ratio (SNR), which is linearly proportional to the imaging field strength. Demonstrated benefits of such increased signal include: 1) higher imaging resolution; 2) shorter imaging time; 3) improved tissue biochemical profiling through MRS; and 4) improved functional data.[87–90] However, susceptibility related artifacts are more pronounced at 3.0T MRI than 1.5T.[88–90] More importantly, 3.0T MRI has an operating frequency of 128 MHz (vs. 64 MHz of 1.5T), leading to higher radiofrequency (rf) energy deposition.[91–93] Specific absorption rate (SAR) measures energy deposition, and is defined as rf power absorbed per unit mass of the tissue (Watts/Kg).[94–96] The issue of increased SAR in pregnancy has limited the use of 3.0T MRI in fetal imaging.[73, 82] Yet, radiofrequency energy deposition (SAR) can be reduced through pulse sequence modifications.[97–100] Therefore, we hypothesized that by using modified pulse sequences, imaging the fetal brain at 3.0T (vs. 1.5T) could be performed at a higher resolution with improved image quality, while simultaneously reducing the SAR.

The objectives of this study were to: 1) evaluate the feasibility of fetal brain magnetic resonance imaging (MRI) using a fast spin echo imaging sequence at 3.0T field strength with simultaneous reduction in radio frequency (rf) energy deposition; 2) quantitatively

compare the image quality with conventional 1.5T MRI; and 3) compare tissue contrast and conspicuity for specific anatomical structures in the brain between 1.5T and 3.0T MRI.

MATERIALS AND METHODS

Pregnant women (19–40 weeks of gestation) scheduled to undergo a 1.5T MR exam for clinical indications were approached to also undergo a 3.0T exam afterwards. All women recruited as part of this study were referred for a clinical MRI through Hutzel Women's Hospital in Detroit, MI. The 1.5T MRI scans were performed at Children's Hospital of Michigan, Detroit, MI, while 3.0T MRI scans were performed at Wayne State University's Magnetic Resonance Research Facility at Detroit Medical Center, Detroit, MI. All women were enrolled in a research protocol approved by the Human Investigation Committee of Wayne State University, and all participants provided written informed consent for the use of MR images for research purposes.

MRI Examination

To compare the image quality and SAR between 1.5T and 3.0T MR, the T2 weighted single shot fast spin echo sequence (SSFSE) was chosen, since it is the most frequently acquired sequence for evaluating fetal anatomy, and has the highest SAR values in typical fetal MRI protocols.[101]

Clinical MRI scans were performed on a 1.5T General Electric Signa system (Milwaukee, WI) with an 8 channel cardiac array and spine receive coils. Following the scout/localizer scans, anatomical data of the fetal brain were acquired using a T2 weighted SSFSE technique with the following imaging parameters (Table 1): repeat time (TR) 1192–1240 milliseconds (msec), echo time (TE) 90 – 240 msec, slice thickness of 4 mm, voxel size 0.93 x 0.93 mm^2 – 1.3 x 1.3 mm^2, and flip angle 90°. Images were obtained sequentially in three planes (axial, coronal, sagittal) relative to the fetal brain. Acquisitions were repeated when fetal motion was encountered.

All 3.0T MRI scans were performed on a 3.0T Siemens Verio system (Erlangen, Germany) with a 6 channel body flex array and spine receive coils. An additional 2 channel flex extremity receive coil was used in some patients having a larger abdominal girth. Following scout/localizer scans, a T2 weighted single shot turbo spin echo sequence with half-Fourier reconstruction (HASTE) was acquired for anatomical purposes. This sequence implementation is essentially the same as SSFSE on the GE system.[102] The following imaging parameters were used for the HASTE sequence: repeat time (TR) 2600–5000 milliseconds (msec), echo time (TE) 139–140 msec, slice thickness of 3 or 4 mm, voxel size 0.87 x 0.87 mm^2 – 1.1 x 1.1 mm^2, and flip angle 75° with hyper-echo acquisition. Images were obtained sequentially in three planes (axial, coronal, sagittal) relative to the fetal brain. Acquisitions were repeated when fetal motion was encountered.

Data Analysis

T2 data was first reviewed for general image quality, including image or motion artifacts. From data collected at a given field strength, the best dataset (defined as a volume without motion or image artifacts) for each anatomical plane relative to the fetal brain was chosen

for further analysis. Each fetus had 3 datasets collected at 1.5T that were compared with the corresponding datasets acquired at 3.0T.

a. Signal to noise ratio (SNR)—Quantitative comparison of image quality was performed by computing the SNR of the fetal brain. For a given fetus, SNR measurements were computed for each T2 dataset. For all cases, SNR was measured by defining a region of interest (ROI) within the white matter, and mean signal was measured from this ROI. Noise was estimated by measuring the signal standard deviation (SD) from a homogenous white matter region within the ROI. SNR was then defined as: ratio of the mean value of the signal from the ROI and SD measured from the homogeneous signal region. For a given dataset, a central slice within the multislice data was first chosen, such that both cerebral hemispheres were clearly visualized. Next, the mean and SD values from two ROIs (one from each cerebral hemisphere) were obtained, and then averaged to minimize the bias due to coil drop-off or non-uniform excitation.[88, 90, 103, 104] Compared to the 1.5T scan, higher resolution data were acquired at 3.0T with a corresponding higher pixel bandwidth. Therefore, the SNR measures were normalized to a fixed voxel volume of 1 mm^3 and a fixed pixel bandwidth of 244 Hz/pixel, so that a direct comparison could be made between SNR measures of the 1.5T and 3.0T data. Finally, SNR measures from the three T2 data acquisitions were averaged to obtain a single SNR measure for each fetus at a given field strength.

b. Specific absorption rate (SAR)—Whole body SAR values, as estimated by the MR system console, were noted from the DICOM[105] (Digital Imaging and Communications in Medicine) image header. For a given patient, SAR values from the three separate views were noted and averaged to obtain a single SAR measure for each patient at a given field strength. It is noteworthy that whole body SAR values are calculated based on maternal physical parameters, which are also the criteria used to assess safety in rf dosimetry studies for fetal imaging.[106–108]

c. Diagnostic image quality and scoring system—Diagnostic image quality was assessed in a blinded fashion for all 1.5T and 3.0T MR images by a senior pediatric neuroradiologist (SM) with more than 10 years of experience with fetal MRI. The following nominal scoring scheme was used: 1) Score 1: images of diagnostic quality without any artifacts; 2) Score 2: images of diagnostic quality, but with minor artifacts or low SNR; and 3) Score 3: images of non-diagnostic quality. Three datasets were evaluated for each fetus, and the best score was used to represent the overall data quality for that fetus respective to the field strength of the image.

d. Comparison of tissue contrast and conspicuity between 1.5T and 3.0T MRI —High soft tissue contrast occurs when different tissues are reflected by different intensity levels in the images.[37] Conspicuity is the property of being clearly discernible.[109, 110] Both tissue contrast and conspicuity of anatomical structures in the fetal brain were compared in a blinded fashion between 1.5T and 3.0T MRI by a senior pediatric neuroradiologist (SM) with more than 10 years of experience with fetal MRI. Specifically, tissue contrast for the fetal cortex, basal ganglia, dentate nucleus, and germinal matrix were

evaluated due to their inherent discernibility. Conspicuity was evaluated for the fetal optic chiasm, basilar artery and vein of Galen due to their small size. Assessment was performed using the following nominal scoring scheme (performance of 3.0T relative to 1.5T): 1) Score 0: inferior; 2) Score 1: same as 1.5T data; 3) Score 2: superior; and 4) NA: not applicable (some structures cannot be visualized due to either early gestational age or pathology). After reviewing all T2 data acquired in different orientations at a given field strength, a single score was assigned (one for tissue contrast and one for conspicuity) for a given fetus.

e. Statistical Analysis—Normality was assessed using the Kolmogorov-Smirnov test and visual plot inspection. Differences in distributions of normalized SNR and SAR were tested using either the paired t-test or its non-parametric equivalent, the Wilcoxon signed rank test, as appropriate. A 5% threshold was used in determining statistical significance. All analyses were performed using SAS version 9.3 (Cary, N.C.).

RESULTS

Twelve pregnant women prospectively underwent both a 1.5T and 3.0T fetal MR examination. Patients were referred for MRI examination due to the presence of fetal congenital anomalies, which included: Dandy Walker malformation (n = 2), mild cerebral ventriculomegaly, hydrocephalus, mega cisterna magna, myelomeningocele, hypoplastic left heart syndrome, distended small bowel loops, congenital heart disease including left heart syndrome, diaphragmatic hernia, cytomegalovirus infection, and monochorionic/diamniotic twins (with one viable fetus). The median (range) age of mothers was 24 (19–34) years. The median (IQR) gestational age at the time of 3.0T scan was 31.4 (27–34.2) weeks, and the median (IQR) time interval between the 1.5T and 3.0T scans was 2.5 (0.75 –5.25) days. All but three women were imaged within 3 days of the 1.5T scan; these women underwent a 3.0T MRI at 12, 19, and 20 days after the first scan.

a. SNR and SAR—Placement of the ROI on the T2 datasets for SNR measurements are shown in Figure 1. For all cases, normalized SNR and SAR measurements for fetal images obtained at 1.5T and 3.0T are depicted in Table 2. The SNR per unit voxel volume of 1 mm^3 (arbitrary units, a.u.) was significantly higher for images obtained using 3.0T than those obtained at 1.5T [median (IQR):4 (3.1–5.6) vs. 3.35 (2.5–3.65), respectively; $p = 0.03$]. Conversely, the whole body SAR value was significantly lower for images obtained at 3.0T than those obtained at 1.5T (mean ± SD: 0.6 ± 0.12 vs. 1.6 ± 0.2 Watt/kg, respectively; $p < 0.0001$) (Figure 2). Even when excluding the three subjects with more than 3 days between the 1.5T and 3.0T scans, such differences remained significant (SNR; $p = 0.03$ and SAR; $p < 0.0001$).

b. Diagnostic Image Quality—Anatomical data sets in different orientations were acquired from all fetuses at both field strengths. The best score was used to represent the overall data quality for a specific fetus. Scores assigned for diagnostic image quality are shown in Table 3. All cases at both field strengths were scored as having diagnostic quality present (Score of 1 or 2). Thus, there was no case which received a Score of 3 (non-diagnostic quality). Of all the cases, 83.3% (10/12) demonstrated equal diagnostic quality

between both field strengths: 1) 75% (9/12) received a Score of 1 at both 1.5T and 3.0T (indicating diagnostic image quality without any artifacts); and 2) 8.3% (1/12) received a Score of 2 at both 1.5T and 3.0T (indicating diagnostic image quality, but with minor artifacts or low SNR). In 16.7% (2/12) cases, images from 3.0T received a Score of 2, while the corresponding images from 1.5T received a Score of 1. Nevertheless, for a given fetus, data from at least one anatomical orientation had diagnostic quality present at both imaging field strengths.

c. Tissue Contrast—Tissue contrast was evaluated and compared between field strengths for four anatomical structures in the fetal brain: cortex, basal ganglia, dentate nucleus and germinal matrix (Table 4). While the cortex could be visualized and evaluated in all 12 fetuses, the basal ganglia and dentate nucleus were each visualized and evaluated in 11 fetuses, and the germinal matrix in 3 fetuses. Some anatomical structures were not visualized due to either early gestational age or the pathologic abnormality, and were scored as NA (not applicable). Thus, a total of 37 scores were assigned. Images of the cortex, basal ganglia, dentate nucleus, and germinal matrix obtained from 3.0T were equal (57%; 21/37), or superior (35%; 13/37) to that of 1.5T for tissue contrast. In 8% (3/37), tissue contrast of the dentate nucleus was inferior on 3.0T (vs. 1.5T) MRI.

d. Conspicuity—Conspicuity was evaluated and compared between field strengths for three fetal anatomical brain structures: optic chiasm, basilar artery and vein of Galen (Table 4). In one fetus, these structures could not be visualized due to early gestational age. Thus a total of 33 scores were assigned. Images of the optic chiasm, basilar artery, and vein of Galen obtained from 3.0T were equal (61%; 20/33) or superior (33%; 11/33) to that of 1.5T for conspicuity. In 6% (2/33), conspicuity of the optic chiasm and basilar artery was inferior on 3.0T (vs. 1.5T) MRI.

Comparisons between MR images of the fetal brain obtained at 1.5T and 3.0T field strengths are shown in Figures 3 through 5. Figure 3 compares images from a 26 week fetus that was scanned on the same day at both field strengths. Figure 4 depicts 1.5T images of the fetal brain and the corresponding 3.0T images of three different fetuses at varying gestational ages. Figure 5 compares the conspicuity and contrast of the germinal matrix, optic nerve, and basilar artery, as well as the migrational pattern seen between 1.5T vs. 3.0T MRI. Superior tissue contrast and conspicuity was observed in the 3.0T images.

DISCUSSION

The principal findings of this study are: 1) SNR was significantly higher for images obtained using 3.0T than those obtained at 1.5T; 2) the average whole body SAR value was significantly lower for images obtained at 3.0T than those obtained at 1.5T; 3) all cases at both field strengths were scored as having diagnostic quality present, and 83.3% of cases demonstrated equal diagnostic quality between both field strengths; 4) images from 3.0T MRI (compared to 1.5T) were equal (57%) or superior (35%) for tissue contrast; and 5) images from 3.0T MRI (compared to 1.5T) were equal (61%) or superior (33%) for conspicuity of anatomical structures. Such superior conspicuity could be attributed, in part, to higher resolution imaging with 3.0T MRI, and changes in the tissue relaxation times

between 1.5 and 3.0T. The smaller voxel size allowed for clearer visualization of certain anatomical structures (e.g. optic nerve) (Figure 5) and thus, improved conspicuity. Tissue T2 relaxation values are known to decrease with increasing field strength. [111–113] Due to the use of almost equivalent echo times between both field strengths, this effectively led to an increased T2 weighting at 3.0T compared to 1.5T, which may have contributed to the improved tissue contrast and conspicuity.

Signal to noise ratio (SNR) in MR imaging is roughly linearly proportional to the imaging field strength, and is one of the main incentives for moving to fetal imaging at 3.0T. Practically, the factor 2 gain in SNR is not always seen at 3.0T due to various factors, such as rf inhomogeneity (excitation and reception) and field appropriate sequence modifications performed for optimizing image quality. In the study herein, additional sequence modifications were employed for SAR reduction. Yet, despite this, we observed a significantly higher SNR at 3.0T than at 1.5T. The higher SNR allowed for higher resolution acquisition at 3.0T (compared to 1.5T), which improved the definition of smaller anatomical structures, such as the optic chiasm.

SAR is a crucial factor to consider when imaging the fetus at 3.0T. Importantly, when imaging the fetal brain at 3.0T, there were lower SAR values (despite better SNR) compared to that of 1.5T (by almost a factor of 2). The SAR values compared in the current study are average whole body SAR values as calculated by the MRI scanner, which assumes certain standard adult imaging conditions.[114] SAR is also dependent on multiple factors, such as body shape, surface area, composition, and spatial location within the scanner. Recent rf dosimetry studies of pregnant human models report that, provided the scanner calculated maternal whole body SAR is < 2W/kg, the local fetal SAR values and tissue temperature increase at 3.0T field strength are well within the safety limits.[106–108] Moreover, the lower the maternal whole body average SAR, the lower is the rf energy deposition in the fetus.[106–108] The SAR parameter also has the following dependency on MR imaging parameters and patient weight:[92, 93, 114, 115]

$$\mathrm{SAR} \propto (\theta)^2 * (1/\mathrm{TR}) * (1/\tau_{\mathrm{rf}}) * (1/\mathrm{W}),$$

where θ is the rf pulse flip angle of the imaging sequence, τ_{rf} is the rf pulse duration, TR is the repetition time of the MR imaging sequence, and W is the weight of the patient. Therefore, SAR is directly proportional to the imaging flip angle, and inversely proportional to the rf pulse duration and TR of the sequence. In this study, a HASTE sequence with hyperecho option was used for imaging at 3.0T.[100, 116–118] Along with the use of lower flip angle pulses of 75°, this hyperecho option helped to reduce rf energy deposition.[100, 116–118] In addition, rf pulses with a longer pulse duration (using the ‘low SAR’ option on the scanner) and a longer TR were used for the HASTE sequence at 3.0T. All of these factors contributed towards significantly lower SAR values at 3.0T compared to 1.5T. The SAR values at 3.0T reported herein, are also lower than those reported by Victoria et al in a recent review paper.[82] Indeed, in the study herein, the maximum SAR for the HASTE sequence at 3.0T field strength was 25% less than the 2 W/Kg limit corresponding to the

'normal' operating mode of clinical MRI scanners.[119, 120] While the lower nominal excitation flip angle does affect the SNR to some extent, this did not significantly reduce the quality of the images at 3.0T, which is evident from the diagnostic image quality scores.

Some limitations of this work include the small sample size and variation in the time duration between 1.5T and 3.0T studies. However, even when excluding the three subjects with more than 3 days between the 1.5T and 3.0T scans, the differences in SNR and SAR between field strengths remained significant and did not alter our findings.

MR imaging at 3.0T offers tremendous advantages in terms of SNR and improved spectral separation in MRS. This could allow the use of faster and more sensitive advanced sequences to image the human fetus (e.g. brain) at 3.0T, such as susceptibility weighted imaging, diffusion weighted imaging, and magnetic resonance spectroscopy, all of which are typically low in SAR.[121]

CONCLUSION

This is the first study in the human fetus to systematically compare SNR, SAR and image quality between 1.5T and 3.0T MRI. With appropriate sequence adaptations, examining the fetal brain using 3.0T MRI results in higher image resolution and SNR, with simultaneously lower radio frequency energy deposition than that of 1.5T. Moreover, 3.0T images demonstrate superior tissue contrast and conspicuity than images obtained using 1.5T MRI in approximately one-thirds of cases.

Acknowledgments

Funding: Wayne State University's Perinatology VirtualDiscovery Grant (made possible by W.K. Kellogg Foundationaward), (Grant/Award Number: 'P3018205') NationalInstitute of Child Health and Human Development,(Grant/Award Number: 'HSN275201300006C') National Heart, Lung, and Blood Institute (NHLBI), (Grant/Award Number: '1R42HL112580-01A1').

This research was supported in part by: the Perinatology Research Branch, Division of Intramural Research, Eunice Kennedy Shriver National Institute of Child Health and Human Development, National Institutes of Health, Department of Health and Human Services (NICHD/NIH); by with Federal funds from NICHD, NIH under Contract No. HSN275201300006C; by the STTR grant from NHLBI (1R42HL112580-01A1); by Wayne State University's Perinatal Research Initiative and by Wayne State University's Perinatology Virtual Discovery Grant (made possible by W.K. Kellogg Foundation award P3018205 to JN).

References

1. Vimercati A, et al. The diagnostic role of "in utero" magnetic resonance imaging. J Perinat Med. 1999; 27(4):303–8. [PubMed: 10560083]
2. Levine D, et al. Placenta accreta: evaluation with color Doppler US, power Doppler US, and MR imaging. Radiology. 1997; 205(3):773–6. [PubMed: 9393534]
3. Hubbard AM, Crombleholme TM, Adzick NS. Prenatal MRI evaluation of giant neck masses in preparation for the fetal exit procedure. Am J Perinatol. 1998; 15(4):253–7. [PubMed: 9565224]
4. Levine D. Ultrasound versus magnetic resonance imaging in fetal evaluation. Top Magn Reson Imaging. 2001; 12(1):25–38. [PubMed: 11215713]
5. Levine D. Magnetic resonance imaging in prenatal diagnosis. Curr Opin Pediatr. 2001; 13(6):572–8. [PubMed: 11753109]
6. Levine D, et al. Central nervous system abnormalities assessed with prenatal magnetic resonance imaging. Obstet Gynecol. 1999; 94(6):1011–9. [PubMed: 10576192]

7. Huisman TA, et al. Fetal magnetic resonance imaging of the central nervous system: a pictorial essay. Eur Radiol. 2002; 12(8):1952–61. [PubMed: 12136313]
8. Sharma G, et al. Use of fetal magnetic resonance imaging in patients electing termination of pregnancy by dilation and evacuation. Am J Obstet Gynecol. 2003; 189(4):990–3. [PubMed: 14586341]
9. Baker PN, et al. A three-year follow-up of children imaged in utero with echo-planar magnetic resonance. Am J Obstet Gynecol. 1994; 170(1 Pt 1):32–3. [PubMed: 8296840]
10. Fenton BW, et al. Magnetic resonance spectroscopy to detect lecithin in amniotic fluid and fetal lung. Obstet Gynecol. 2000; 95(3):457–60. [PubMed: 10711563]
11. Duncan K, Baker P, Johnson I. The complementary role of echoplanar magnetic resonance imaging and three-dimensional ultrasonography in fetal lung assessment. Am J Obstet Gynecol. 1997; 177(1):244–5. [PubMed: 9240616]
12. Duncan KR, et al. The investigation of placental relaxation and estimation of placental perfusion using echo-planar magnetic resonance imaging. Placenta. 1998; 19(7):539–43. [PubMed: 9778128]
13. Duncan KR, et al. Assessment of fetal lung growth in utero with echo-planar MR imaging. Radiology. 1999; 210(1):197–200. [PubMed: 9885608]
14. Baker PN, et al. Estimation of fetal lung volume using echo-planar magnetic resonance imaging. Obstet Gynecol. 1994; 83(6):951–4. [PubMed: 8190438]
15. Langer B, et al. Low-field dedicated magnetic resonance imaging: a potential tool for assisting perinatal autopsy. Ultrasound Obstet Gynecol. 1998; 12(4):271–5. [PubMed: 9819860]
16. Malinger G, et al. Fetal brain imaging: a comparison between magnetic resonance imaging and dedicated neurosonography. Ultrasound Obstet Gynecol. 2004; 23(4):333–40. [PubMed: 15065181]
17. Malinger G, Lev D, Lerman-Sagie T. Is fetal magnetic resonance imaging superior to neurosonography for detection of brain anomalies? Ultrasound Obstet Gynecol. 2002; 20(4):317–21. [PubMed: 12383310]
18. Manganaro L, et al. Role of foetal MRI in the evaluation of ischaemic-haemorrhagic lesions of the foetal brain. Journal of Perinatal Medicine. 2012; 40(4):419–426. [PubMed: 22752774]
19. Manganaro L, et al. Fetal MRI with diffusion-weighted imaging (DWI) and apparent diffusion coefficient (ADC) assessment in the evaluation of renal development: preliminary experience in normal kidneys. Radiologia Medica. 2009; 114(3):403–13. [PubMed: 19381763]
20. Manganaro L, et al. Diffusion-weighted MR imaging and apparent diffusion coefficient of the normal fetal lung: preliminary experience. Prenatal Diagnosis. 2008; 28(8):745–748. [PubMed: 18567059]
21. Johnson IR, et al. Study of internal structure of the human fetus in utero by echo-planar magnetic resonance imaging. Am J Obstet Gynecol. 1990; 163(2):601–7. [PubMed: 2386150]
22. Gowland PA, et al. In vivo relaxation time measurements in the human placenta using echo planar imaging at 0.5 T. Magn Reson Imaging. 1998; 16(3):241–7. [PubMed: 9621965]
23. Alderliesten ME, et al. Perinatal mortality: clinical value of postmortem magnetic resonance imaging compared with autopsy in routine obstetric practice. BJOG. 2003; 110(4):378–82. [PubMed: 12699799]
24. Huisman TA, et al. MR autopsy in fetuses. Fetal Diagn Ther. 2002; 17(1):58–64. [PubMed: 11803219]
25. Meyer-Wittkopf M, et al. Evaluation of three-dimensional ultrasonography and magnetic resonance imaging in assessment of congenital heart anomalies in fetal cardiac specimens. Ultrasound Obstet Gynecol. 1996; 8(5):303–8. [PubMed: 8978001]
26. Lee W, et al. A diagnostic approach for the evaluation of spina bifida by three-dimensional ultrasonography. J Ultrasound Med. 2002; 21(6):619–26. [PubMed: 12054297]
27. Lee W, et al. Non-invasive fetal lung assessment using diffusion-weighted imaging. Ultrasound in Obstetrics & Gynecology. 2009; 34(6):673–677. [PubMed: 19859908]
28. Kok RD, et al. Decreased relative brain tissue levels of inositol in fetal hydrocephalus. Am J Obstet Gynecol. 2003; 188(4):978–80. [PubMed: 12712096]

29. Kadri M, et al. Proton magnetic resonance spectroscopy improves outcome prediction in perinatal CNS insults. J Perinatol. 2003; 23(3):181–5. [PubMed: 12732853]
30. Emamian SA, et al. Fetal MRI evaluation of an intracranial mass: in utero evolution of hemorrhage. Pediatr Radiol. 2002; 32(8):593–7. [PubMed: 12136352]
31. Kathary N, et al. MRI imaging of fetal neck masses with airway compromise: utility in delivery planning. Pediatr Radiol. 2001; 31(10):727–31. [PubMed: 11685443]
32. Tanaka YO, et al. High temporal resolution dynamic contrast MRI in a high risk group for placenta accreta. Magn Reson Imaging. 2001; 19(5):635–42. [PubMed: 11672621]
33. Regan F, Cavaluzzi J, Nguyen B. Fast MR abdominal imaging using the HASTE sequence. AJR Am J Roentgenol. 1998; 170(6):1471–6. [PubMed: 9609155]
34. Yamashita Y, et al. MR imaging of the fetus by a HASTE sequence. AJR Am J Roentgenol. 1997; 168(2):513–9. [PubMed: 9016238]
35. Whitby EH, et al. Comparison of ultrasound and magnetic resonance imaging in 100 singleton pregnancies with suspected brain abnormalities. BJOG. 2004; 111(8):784–92. [PubMed: 15270925]
36. Laurichesse Delmas H, et al. Prenatal diagnosis of thrombosis of the dural sinuses: report of six cases, review of the literature and suggested management. Ultrasound Obstet Gynecol. 2008; 32(2):188–98. [PubMed: 18512853]
37. Powell MC, et al. Magnetic resonance imaging (MRI) in obstetrics. II. Fetal anatomy. Br J Obstet Gynaecol. 1988; 95(1):38–46. [PubMed: 3342208]
38. Mansfield P, et al. Echo planar imaging of the human fetus in utero at 0.5 T. Br J Radiol. 1990; 63(755):833–41. [PubMed: 2252974]
39. Stehling MK, et al. Echo-planar imaging of the human fetus in utero. Magn Reson Med. 1990; 13(2):314–8. [PubMed: 2314220]
40. Baldoli C, et al. Demonstration of acute ischemic lesions in the fetal brain by diffusion magnetic resonance imaging. Ann Neurol. 2002; 52(2):243–6. [PubMed: 12210800]
41. Guimiot F, et al. Contribution of diffusion-weighted imaging in the evaluation of diffuse white matter ischemic lesions in fetuses: correlations with fetopathologic findings. AJNR Am J Neuroradiol. 2008; 29(1):110–5. [PubMed: 17947368]
42. Righini A, et al. Diffusion-weighted magnetic resonance imaging of acute hypoxic-ischemic cerebral lesions in the survivor of a monochorionic twin pregnancy: case report. Ultrasound Obstet Gynecol. 2007; 29(4):453–6. [PubMed: 17390325]
43. Oubel E, et al. Reconstruction of scattered data in fetal diffusion MRI. Med Image Comput Comput Assist Interv. 2010; 13(Pt 1):574–81. [PubMed: 20879277]
44. Oubel E, et al. Reconstruction of scattered data in fetal diffusion MRI. Med Image Anal. 2012; 16(1):28–37. [PubMed: 21636311]
45. Oubel, E., et al. Evaluation of different strategies for distortion correction in fetal diffusion-weighted imaging. MICCAI workshop: Image Analysis for the Developing Brain; 2009; London, U.K.
46. Jiang S, et al. In-utero three dimension high resolution fetal brain diffusion tensor imaging. Med Image Comput Comput Assist Interv. 2007; 10(Pt 1):18–26.
47. Jiang S, et al. Diffusion tensor imaging (DTI) of the brain in moving subjects: application to in-utero fetal and ex-utero studies. Magn Reson Med. 2009; 62(3):645–55. [PubMed: 19526505]
48. Moore RJ, et al. In vivo diffusion measurements as an indication of fetal lung maturation using echo planar imaging at 0.5T. Magnetic Resonance in Medicine. 2001; 45(2):247–253. [PubMed: 11180432]
49. Moore RJ, et al. In utero perfusing fraction maps in normal and growth restricted pregnancy measured using IVIM echo-planar MRI. Placenta. 2000; 21(7):726–32. [PubMed: 10985977]
50. Francis ST, et al. Non-invasive mapping of placental perfusion. Lancet. 1998; 351(9113):1397–9. [PubMed: 9593410]
51. Moore RJ, et al. Antenatal determination of fetal brain activity in response to an acoustic stimulus using functional magnetic resonance imaging. Hum Brain Mapp. 2001; 12(2):94–99. [PubMed: 11169873]

52. Wedegartner U, et al. Functional MR imaging: comparison of BOLD signal intensity changes in fetal organs with fetal and maternal oxyhemoglobin saturation during hypoxia in sheep. Radiology. 2006; 238(3):872–80. [PubMed: 16439569]
53. Fulford J, et al. Fetal brain activity in response to a visual stimulus. Hum Brain Mapp. 2003; 20(4): 239–45. [PubMed: 14673807]
54. Gowland P, Fulford J. Initial experiences of performing fetal fMRI. Exp Neurol. 2004; 190(Suppl 1):S22–7. [PubMed: 15498538]
55. Thomason ME, et al. Cross-hemispheric functional connectivity in the human fetal brain. Sci Transl Med. 2013; 5(173):173ra24.
56. van Cappellen van Walsum AM, et al. Proton magnetic resonance spectroscopy of fetal lamb brain during hypoxia. Am J Obstet Gynecol. 1998; 179(3 Pt 1):756–7. [PubMed: 9757984]
57. Fenton BW, et al. The fetus at term: in utero volume-selected proton MR spectroscopy with a breath-hold technique--a feasibility study. Radiology. 2001; 219(2):563–6. [PubMed: 11323489]
58. Girard N, et al. MRS of normal and impaired fetal brain development. Eur J Radiol. 2006; 57(2): 217–25. [PubMed: 16387464]
59. Kimura H, et al. Metabolic alterations in the neonate and infant brain during development: evaluation with proton MR spectroscopy. Radiology. 1995; 194(2):483–9. [PubMed: 7529934]
60. Girard N, et al. Assessment of normal fetal brain maturation in utero by proton magnetic resonance spectroscopy. Magn Reson Med. 2006; 56(4):768–75. [PubMed: 16964617]
61. Brighina E, et al. Human Fetal Brain Chemistry as Detected by Proton Magnetic Resonance Spectroscopy. Pediatr Neurol. 2009; 40(5):327–342. [PubMed: 19380068]
62. Cetin I, et al. Lactate detection in the brain of growth-restricted fetuses with magnetic resonance spectroscopy. Am J Obstet Gynecol. 2011; 205(4):350 e1–7. [PubMed: 21861968]
63. Clouchoux C, Limperopoulos C. Novel applications of quantitative MRI for the fetal brain. Pediatr Radiol. 2012; 42:24–32. [PubMed: 22179682]
64. Heerschap A, Kok RD, van den Berg PP. Antenatal proton MR spectroscopy of the human brain in vivo. Childs Nerv Syst. 2003; 19(7–8):418–21. [PubMed: 12811484]
65. Kok RD, et al. Maturation of the human fetal brain as observed by H-1 MR spectroscopy. Magnetic Resonance in Medicine. 2002; 48(4):611–616. [PubMed: 12353277]
66. Nemec SF, et al. Abnormalities of the penis in utero--hypospadias on fetal MRI. J Perinat Med. 2011; 39(4):451–6. [PubMed: 21631398]
67. Matsuda H, et al. Cerebral edema on MRI in severe preeclamptic women developing eclampsia. J Perinat Med. 2005; 33(3):199–205. [PubMed: 15914341]
68. Ikeda K, et al. Intrauterine MRI with single-shot fast-spin echo imaging showed different signal intensities in hypoplastic lungs. J Perinat Med. 2000; 28(2):151–4. [PubMed: 10875102]
69. Trop I, Levine D. Normal fetal anatomy as visualized with fast magnetic resonance imaging. Top Magn Reson Imaging. 2001; 12(1):3–17. [PubMed: 11215714]
70. Levine, D. Atlas of fetal MRI. Boca Raton: Taylor & Francis; 2005. p. xip. 2391 online resource
71. Levine D, et al. Fetal central nervous system anomalies: MR imaging augments sonographic diagnosis. Radiology. 1997; 204(3):635–42. [PubMed: 9280237]
72. Kubik-Huch RA, et al. Ultrafast MR imaging of the fetus. AJR Am J Roentgenol. 2000; 174(6): 1599–606. [PubMed: 10845491]
73. Prayer, D. Fetal MRI. Springer; 2011.
74. Debillon T, et al. Limitations of ultrasonography for diagnosing white matter damage in preterm infants. Arch Dis Child Fetal Neonatal Ed. 2003; 88(4):F275–9. [PubMed: 12819157]
75. Inder TE, et al. White matter injury in the premature infant: a comparison between serial cranial sonographic and MR findings at term. AJNR Am J Neuroradiol. 2003; 24(5):805–9. [PubMed: 12748075]
76. Jung E, et al. Spontaneous resolution of prenatally diagnosed dural sinus thrombosis: a case report. Ultrasound Obstet Gynecol. 2006; 27(5):562–5. [PubMed: 16586467]
77. Ghi T, et al. Outcome of antenatally diagnosed intracranial hemorrhage: case series and review of the literature. Ultrasound Obstet Gynecol. 2003; 22(2):121–30. [PubMed: 12905503]

78. Smith FW, Adam AH, Phillips WD. NMR imaging in pregnancy. Lancet. 1983; 1(8314–5):61–2. [PubMed: 6129387]

79. Filippi, CG., et al. Fetal Imaging with Multitransmit MR at 3.0T: Preliminary Findings. Joint Annual Meeting ISMRM-ESMRMB; 2010; Stockholm, Sweden. 2010. Poster# 2023

80. Barr SM, et al. Assessment of intra-hepatic and intra-muscular lipid in obese pregnant women: an application of 3-tesla MRI. Archives of Disease in Childhood - Fetal and Neonatal Edition. 2011; 96(Suppl 1):Fa118.

81. Welsh RC, Nemec U, Thomason ME. Fetal magnetic resonance imaging at 3.0 T. Top Magn Reson Imaging. 2011; 22(3):119–31. [PubMed: 23558467]

82. Victoria T, et al. Fetal magnetic resonance imaging: jumping from 1.5 to 3 tesla (preliminary experience). Pediatr Radiol. 2014; 44(4):376–86. [PubMed: 24671739]

83. Wardlaw JM, et al. A systematic review of the utility of 1.5 versus 3 Tesla magnetic resonance brain imaging in clinical practice and research. European Radiology. 2012; 22(11):2295–2303. [PubMed: 22684343]

84. Wood R, et al. 1.5 tesla magnetic resonance imaging scanners compared with 3.0 tesla magnetic resonance imaging scanners: systematic review of clinical effectiveness. CADTH Technol Overv. 2012; 2(2):e2201. [PubMed: 23002376]

85. Knickmeyer RC, et al. A structural MRI study of human brain development from birth to 2 years. J Neurosci. 2008; 28(47):12176–82. [PubMed: 19020011]

86. Gilmore JH, et al. 3 Tesla magnetic resonance imaging of the brain in newborns. Psychiatry Res. 2004; 132(1):81–5. [PubMed: 15546705]

87. Alvarez-Linera J. 3T MRI: advances in brain imaging. Eur J Radiol. 2008; 67(3):415–26. [PubMed: 18455895]

88. Machann J, Schlemmer HP, Schick F. Technical challenges and opportunities of whole-body magnetic resonance imaging at 3T. Phys Med. 2008; 24(2):63–70. [PubMed: 18308606]

89. Soher BJ, Dale BM, Merkle EM. A review of MR physics: 3T versus 1.5T. Magn Reson Imaging Clin N Am. 2007; 15(3):277–90. v. [PubMed: 17893049]

90. Akisik FM, et al. Abdominal MR Imaging at 3.0 T. Radiographics. 2007; 27(5)

91. Hoult DI. Sensitivity and power deposition in a high-field imaging experiment. Journal of Magnetic Resonance Imaging. 2000; 12(1):46–67. [PubMed: 10931564]

92. Hoult DI, Lauterbur PC. Sensitivity of the Zeugmatographic Experiment Involving Human Samples. J Magn Reson. 1979; 34(2):425–433.

93. Roschmann P. Radiofrequency Penetration and Absorption in the Human-Body - Limitations to High-Field Whole-Body Nuclear-Magnetic-Resonance Imaging. Med Phys. 1987; 14(6):922–931. [PubMed: 3696080]

94. Institute of Electrical and Electronic Engineers (IEEE). IEEE C95.3–2002. New York: IEEE; 2002. IEEE recommended practice for measurements and computations of radio frequency electromagnetic fields with respect to human exposure to such fields, 100 kHz– 300 GHz.

95. International Commission on Non-Ionizing Radiation Protection (ICNIRP). ICNIRP statement on the ‘Guidelines for limiting exposure to time-varying electric, magnetic, and electromagnetic fields (up to 300 GHz)’. Health Physics. 2009a; 97:257–258. [PubMed: 19667809]

96. International Commission on Non-Ionizing Radiation Protection (ICNIRP). Amendment to the ICNIRP ‘Statement on medical Magnetic Resonance (MR) procedures: protection of patients’. Health Physics. 2009b; 97:259–61. [PubMed: 19667810]

97. Neelavalli J. T1 and susceptibility contrast at high fields. 2008:110.

98. Sarkar SN, et al. Brain MR Imaging at Ultra-low Radiofrequency Power. Radiology. 2011; 259(2): 550–557. [PubMed: 21357520]

99. Busse RF. Reduced RF power without blurring: Correcting for modulation of refocusing flip angle in FSE sequences. Magnetic Resonance in Medicine. 2004; 51(5):1031–1037. [PubMed: 15122687]

100. Hennig J, Weigel M, Scheffler K. Multiecho sequences with variable refocusing flip angles: Optimization of signal behavior using smooth transitions between pseudo steady states (TRAPS). Magnetic Resonance in Medicine. 2003; 49(3):527–535. [PubMed: 12594756]

101. Brugger PC, Prayer D. Actual imaging time in fetal MRI. Eur J Radiol. 2012; 81(3):e194–6. [PubMed: 21345632]
102. Elmaoğlu, M., Çelik, A. MRI handbook : MR physics, patient positioning, and protocols. New York: Springer; 2012. p. xiip. 318
103. Hussain SM, et al. MR imaging of the female pelvis at 3T. Magn Reson Imaging Clin N Am. 2006; 14(4):537–44. vii. [PubMed: 17433982]
104. Kataoka M, et al. MR imaging of the female pelvis at 3 Tesla: Evaluation of image homogeneity using different dielectric pads. Journal of Magnetic Resonance Imaging. 2007; 26(6):1572–1577. [PubMed: 17968958]
105. National Electrical Manufacturers Association. and American College of Radiology. Digital imaging and communications in medicine (DICOM). Vol. v. Washington, D.C: National Electrical Manufacturers Association; 1998. p. 1-8.p. 10-15.
106. Hand J, Li Y, Hajnal J. Numerical study of RF exposure and the resulting temperature rise in the foetus during a magnetic resonance procedure. Physics in medicine and biology. 2010; 55(4):913. [PubMed: 20090188]
107. Kikuchi S, et al. Temperature elevation in the fetus from electromagnetic exposure during magnetic resonance imaging. Phys Med Biol. 2010; 55(8):2411–26. [PubMed: 20360633]
108. Hirata A, et al. The relationship between specific absorption rate and temperature elevation in anatomically based human body models for plane wave exposure from 30 MHz to 6 GHz. Physics in medicine and biology. 2013; 58(4):903. [PubMed: 23337764]
109. Levine D, et al. Fetal fast MR imaging: reproducibility, technical quality, and conspicuity of anatomy. Radiology. 1998; 206(2):549–54. [PubMed: 9457211]
110. Troiano RN, Lange RC, McCarthy S. Conspicuity of normal and pathologic female pelvic anatomy: comparison of gadolinium-enhanced T1-weighted images and fast spin echo T2-weighted images. J Comput Assist Tomogr. 1996; 20(6):871–7. [PubMed: 8933784]
111. Bottomley PA, et al. A Review of Normal Tissue Hydrogen Nmr Relaxation-Times and Relaxation Mechanisms from 1–100 Mhz - Dependence on Tissue-Type, Nmr Frequency, Temperature, Species, Excision, and Age. Med Phys. 1984; 11(4):425–448. [PubMed: 6482839]
112. Stanisz GJ, et al. T-1, T-2 relaxation and magnetization transfer in tissue at 3T. Magnetic Resonance in Medicine. 2005; 54(3):507–512. [PubMed: 16086319]
113. Wansapura JP, et al. NMR relaxation times in the human brain at 3.0 tesla. Jmri-Journal of Magnetic Resonance Imaging. 1999; 9(4):531–538.
114. Wang ZW, Lin JC. SAR Calculations in MRI Scanning Systems. Ieee Microwave Magazine. 2012; 13(5):22–29.
115. Edelstein WA, et al. The Intrinsic Signal-to-Noise Ratio in Nmr Imaging. Magnetic Resonance in Medicine. 1986; 3(4):604–618. [PubMed: 3747821]
116. Kiefer B, Grassner J, Hausman K. Image acquisition in a second with half Fourier acquisition single shot turbo spin echo. J Magn Reson Imaging. 1994; 4(P):86.
117. Semelka RC, et al. HASTE MR imaging: description of technique and preliminary results in the abdomen. J Magn Reson Imaging. 1996; 6(4):698–9. [PubMed: 8835965]
118. Hennig J, Scheffler K. Hyperechoes. Magn Reson Med. 2001; 46(1):6–12. [PubMed: 11443704]
119. A Primer on Medical Device Interactions with Magnetic Resonance Imaging Systems. 1997. Available from: http://www.fda.gov/MedicalDevices/DeviceRegulationandGuidance/GuidanceDocuments/ucm107721.htm
120. Guidance for Industry and FDA Staff: Criteria for Significant Risk Investigations of Magnetic Resonance Diagnostic Devices. 2003. Available from: http://www.fda.gov/MedicalDevices/DeviceRegulationandGuidance/GuidanceDocuments/ucm072686.htm
121. Brugger PC, Prayer D. Actual imaging time in fetal MRI. Eur J Radiol. 2012; 81(3):E194–E196. [PubMed: 21345632]

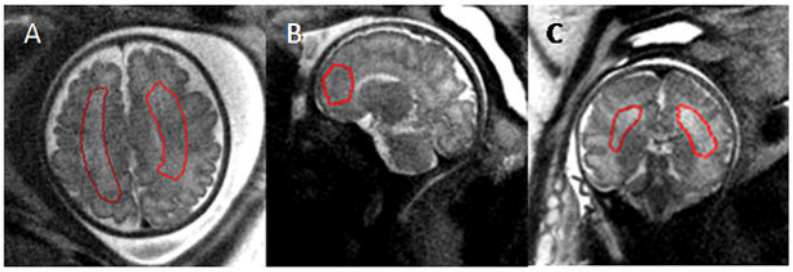

Figure 1.

Placement of the ROI on T2 MRI datasets. ROIs were drawn on data acquired in three orientations for SNR measurements. Gestational age (weeks) A: 34 1/7; B: 34 4/7; C: 22 3/7. Images shown were acquired at 3.0T field strength.

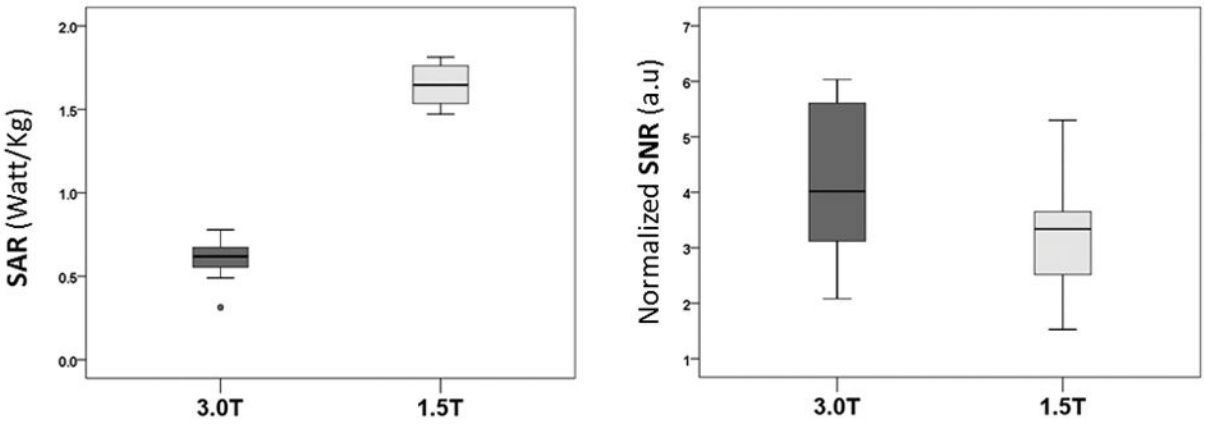

Figure 2.

Comparison of normalized SAR and SNR values between T2 weighted single shot fast spin echo (SSFSE) sequence data obtained at 1.5T and 3.0T fetal MRI field strengths. (a.u., arbitrary units).

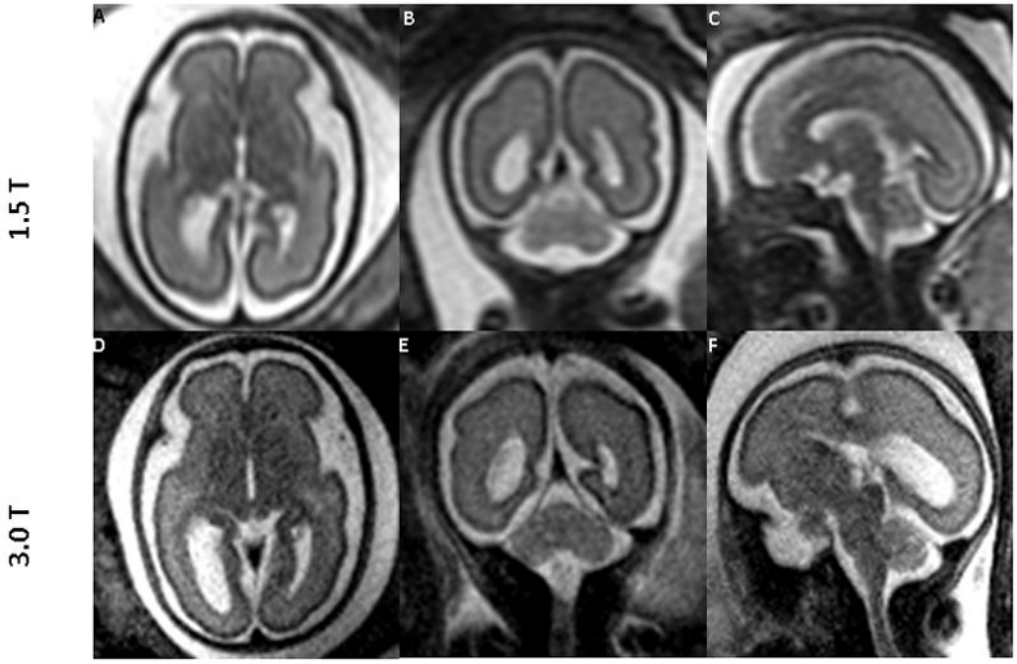

Figure 3.

Comparing images of the fetal brain at 26 weeks of gestation obtained at 1.5T and 3.0T MRI (same fetus): 1.5T (top row, A–C) and 3.0T (bottom row, D–F) in all three orientations: Axial (A,D); Sagittal (B,E); and Coronal (C,F). Both 1.5T and 3.0T scans were performed on the same day. The images from 3.0T show superior tissue contrast and conspicuity to that of 1.5T.

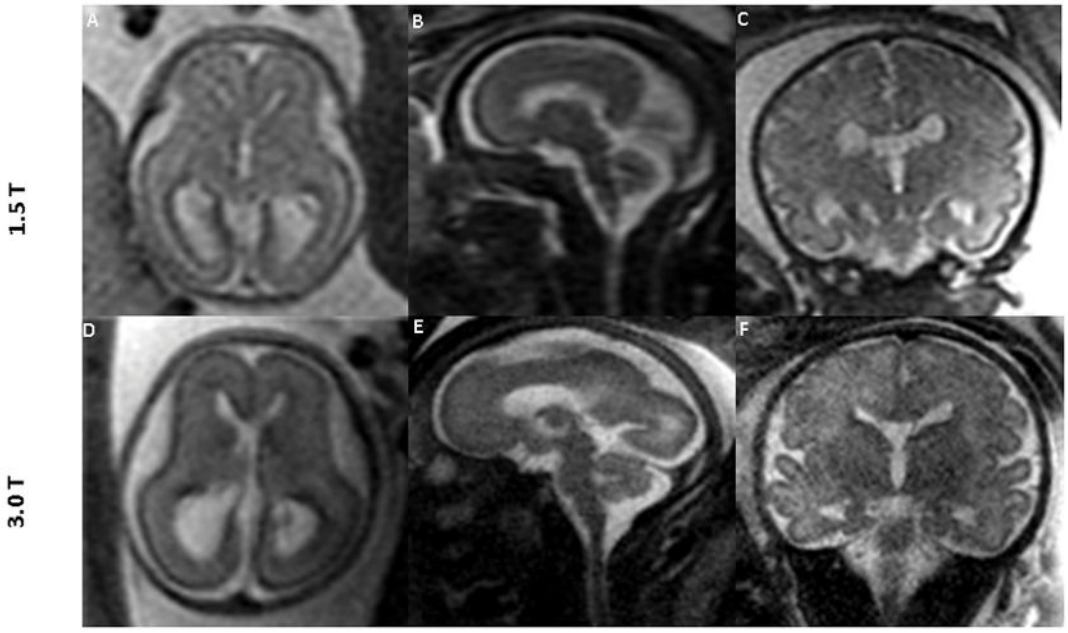

Figure 4.

1.5T MR images of the fetal brain (top row) and the corresponding 3.0T images (bottom row) across different gestational ages. Data were obtained from 3 different fetuses. Images in the top row and the corresponding images in the bottom row are from the same fetus. Gestational age (weeks) at the time of scan were: (A: 22, D: 22 3/7); (B: 27, E: 27 2/7); and (C and F: 35 1/7). Superior tissue contrast and conspicuity is demonstrated in the 3.0T images.

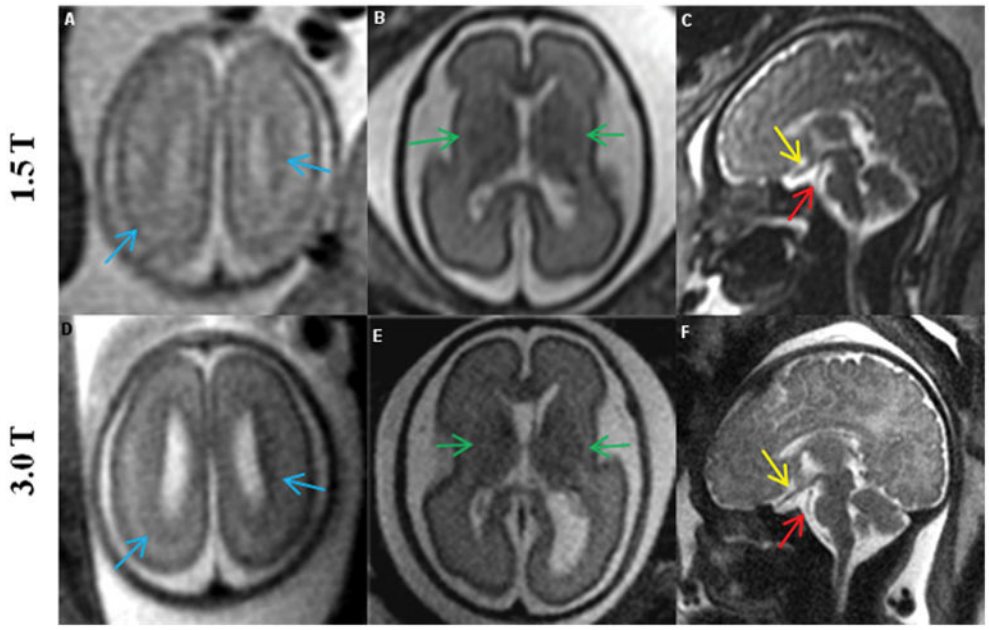

Figure 5.

Comparison of 1.5T (top row) vs. corresponding 3.0T (bottom row) MR images of the fetal brain, showing the advantages of increased resolution at 3.0T. 1) Blue arrows (A, D) show the pattern of migration more clearly at 3.0T; 2) green arrows (B, E) show increased contrast in the germinal matrix; and 3) yellow and red arrows (C, F) show clear delineation of the optic nerve and basilar artery, respectively, at 3.0T. Images in the top row and the corresponding images in the bottom row are from the same fetus. Gestational age (weeks) at the time of scan were: (A: 22, D: 22 3/7); (B and E: 26 1/7) ; (C: 35 1/7, F: 35 4/7).

Table 1

MR imaging parameters for the single shot fast spin echo (SSFSE) sequence at 1.5T and 3.0T

Field Strength	TE (msec)	TR (msec)	Resolution (mm^3)	Flip Angle (degree)	Band width (Hz/pixel)
1.5 T	90 – 240	1192–1240	(0.93 to 1.3) x (0.93 to 1.3) x 4	90	244
3.0 T	139–140	2600–5000	(0.87 to 1.1) x (0.87 to 1.1) x (3 to 4)	75	369 or 372

Table 2

Comparison of normalized signal to noise ratio (SNR, arbitrary units) per unit voxel volume of 1 mm^3 and specific absorption rate (SAR, Watt/Kg) between T2 weighted single shot fast spin echo sequence data (n=12 subjects) obtained at 1.5T and 3.0T fetal MRI field strengths.

	1.5T		3.0T	
Subject #	**SNR (a.u.)**	**SAR (Watt/kg)**	**SNR (a.u.)**	**SAR (Watt/kg)**
1	3.2	1.1	5.5	0.6
2	3.4	1.8	2.1	0.3
3	2.0	1.8	3.1	0.7
4	1.5	1.8	3.7	0.5
5	3.4	1.5	5.3	0.7
6	3.4	1.7	5.8	0.5
7	5.3	1.7	5.7	0.6
8	2.3	1.7	4.3	0.7
9	2.7	1.5	3.6	0.6
10	3.9	1.5	2.9	0.7
11	3.3	1.5	3.1	0.8
12	3.9	1.5	6.0	0.6
Mean (SD)		1.6[*] (0.2)		0.6[*] (0.1)
Median (IQR)	3.35[†] (0.9)		4[†] (2.4)	

[*] P-value < 0.0001

[†] P-value = 0.03

Table 3

Scores assigned for diagnostic image quality for fetal images obtained at 1.5T and 3.0T MRI. The best score was used to represent the overall data quality for a specific fetus.

Diagnostic Image Quality Score		
Subject #	**3.0T**	**1.5T**
1	2	1
2	2	1
3	1	1
4	1	1
5	1	1
6	1	1
7	1	1
8	1	1
9	1	1
10	2	2
11	1	1
12	1	1

Score 1: images of diagnostic quality without any artifacts

Score 2: images of diagnostic quality, but with minor artifacts or low SNR

Score 3: images of non-diagnostic quality

Table 4

Comparison of tissue contrast and conspicuity for anatomical structures in the fetal brain between 1.5T and 3.0T MRI data. Images are scored with regards to how 3.0T compares to 1.5T MRI (reference).

	Tissue contrast				Conspicuity		
	Cortex	**Basal Ganglia**	**Dentate Nucleus**	**Germinal Matrix**	**Optic Chiasm**	**Basilar Artery**	**Vein of Galen**
Inferior (Score 0)	0	0	3	0	1	1	0
Equal (Score 1)	6	7	5	3	6	7	7
Superior (Score 2)	6	4	3	0	4	3	4
NA	0	1	1	9	1	1	1